Available online at www.sciencedirect.com
SCIENCE DIRECT®
ELSEVIER
Palaeogeography, Palaeoclimatology, Palaeoecology 237 (2006) 396–411
PALAEO
www.elsevier.com/locate/palaeo

Forest re-growth on medieval farmland after the Black Death pandemic—Implications for atmospheric CO_2 levels

Thomas B. van Hoof [a,*], Frans P.M. Bunnik [b], Jean G.M. Waucomont [a], Wolfram M. Kürschner [a], Henk Visscher [a]

[a] *Laboratory of Palaeobotany and Palynology, Department of Biology, Faculty of Science, Budapestlaan 4, 3584 CD, Utrecht University, The Netherlands*
[b] *TNO-Geological Survey of the Netherlands, P.O. Box 80015, 3508 TA, Utrecht, The Netherlands*

Received 24 February 2005; received in revised form 13 December 2005; accepted 16 December 2005

Abstract

Well-dated pollen assemblages from an organic-rich infill of an oxbow lake of the river Roer (southeastern Netherlands) provide a high-resolution reconstruction of regional vegetation development and land-use for the period between AD 1000 and 1500. Regional effects of the mid-14th century plague pandemic known as the Black Death are reflected by a period of significant agricultural regression between AD 1350 and 1440. Concomitant re-growth of forest indicates the existence of a terrestrial carbon sink following the Black Death pandemic. A direct temporal correlation of the reconstructed changes in land-cover with a proxy record of atmospheric CO_2 mixing ratios based on stomatal frequency analysis of *Quercus robur* leaf remains suggests the coupling of long-term CO_2 trends of the 13th–15th centuries and coeval trends in regional forest density. During the period of maximum reforestation between AD 1400 and 1440, CO_2 levels seem to be relatively low, but the onset of a CO_2 decline may predate the spread of the Black Death in Europe.

Keywords: Last millennium; Vegetation history; Atmospheric CO_2; Pandemics

1. Introduction

It was recently hypothesized that anthropogenic greenhouse gas forcing has significantly influenced the global climate since about 8000 years BP, when early agriculture began to extend in previously forested regions of Eurasia (Rudimann, 2003). Prior to the industrial revolution, progressive forest clearance could have been responsible for the 20–25 ppmv increase of the atmospheric CO_2 mixing ratios detected in Antarctic ice-core records (Indermühle et al., 1999). Superimposed on this long-term trend, recorded negative CO_2 anomalies of 4–10 ppmv during the past 2000 years (Indermühle et al., 1999) could offer evidence of periodic carbon sequestration possibly due to reforestation of abandoned farmlands following pandemics of plague and other diseases, when the human population was decimated in various parts of the world (Rudimann, 2003).

CO_2 emission data of the 20th century may confirm that extensive forest re-growth of previously logged mid- and high-latitude terrains acted as a sink for anthropogenic CO_2 during the past century (Mellilo et al., 1988; Houghton and Skole, 1990; Dixon et al., 1994; Caspersen et al., 2000). Model simulations suggest that reforestation and afforestation over the next 50

* Corresponding author. Tel.: +31 302539318; fax: +31 302535096.
E-mail address: T.B.vanHoof@bio.uu.nl (T.B. van Hoof).

0031-0182/$ - see front matter © 2005 Elsevier B.V. All rights reserved.
doi:10.1016/j.palaeo.2005.12.013

years would result in a slowdown of the rate of atmospheric CO_2 increase by 15–30 ppmv (House et al., 2002). Because of the coupling between atmospheric CO_2 and global temperature, Rudimann's (2003) theory suggests that pandemic-driven changes in the terrestrial carbon sink could have played an important role in climate variability during the past millennium.

In order to test whether or not forest re-growth on deserted farmland could sequester sufficient carbon to account for atmospheric CO_2 decline, it is essential to obtain information on the nature, timing and magnitude of land-cover changes triggered by massive depopulation events. The largest plague outbreak in European history, the 'Black Death', swept through Europe between AD 1347 and 1350 (e.g. Cartwright, 1972; Taylor, 1983; Bray, 1996; Fagan, 2000; Vasold, 2003). Most historians agree that in various parts of Europe, the Black Death killed 30–45% of the population. There is historical evidence of widespread abandonment of farms and rural villages for decades. Pollen records also reflect changes in the level of agricultural activities during the 14th century. For example, an overall decrease in the frequency of pollen of cultivated plants, notably cereals, has long been apparent (e.g. Overbeck and Griez, 1954; Phillippi, 1965). However, accurate correlation of palynologically identified land-cover changes with well-dated historical events such as the Black Death is difficult. During the last century, extensive drainage of wetland areas in Europe has destroyed or disturbed peat and lake deposits that could yield high-resolution pollen records for the past millennium. To detect direct effects of the Black Death in pollen diagrams covering the period from AD 1350 to 1450, a resolution of 10–20 years would be required.

In the southeastern part of The Netherlands, fluvio-lacustrine sediments, such as channel deposits of oxbow lakes, show intervals with high sedimentation rates and may therefore be suitable for such high-resolution palynological studies. In the vicinity of Sint Odiliënberg (Province of Limburg) we successfully cored an organic-rich infill of an oxbow lake of the river Roer. AMS ^{14}C dating of buried leaf remains indicates that the cores include a continuous sedimentary record for the period between AD 1000 and 1500. In order to obtain insight in the nature and precise timing of effects of the Black Death and its aftermath on regional vegetation and land-use, we present a high-resolution (10–20 years) palynological analysis of this core section. A time-framework for the section is established by ^{14}C wiggle-match dating.

At present, Holocene atmospheric CO_2 reconstructions are not only available from direct measurements of air enclosures in Antarctic ice, but, alternatively, also from stomatal frequency analysis performed on leaves buried in peat and lake deposits. A wide variety of tree species is capable of sustained adjustment of the number of leaf stomata to changing ambient CO_2 mixing ratios (e.g., Woodward, 1987; Kürschner, 1996; Wagner et al., 1996; Royer, 2001). Calibrated against modern training sets, high-resolution stomatal frequency records from Holocene sections all over the Northern Hemisphere, consistently suggest that century-scale CO_2 fluctuations have contributed to a much more dynamic CO_2 evolution than indicated by ice-core measurements (Wagner et al., 1999; Rundgren and Beerling, 1999; McElwain et al., 2002; Wagner et al., 2002; Rundgren and Björck, 2003; Kouwenberg et al., 2005; Jessen et al., 2005; van Hoof et al., 2005). Although representing an indirect proxy for atmospheric CO_2, stomatal frequency data have the major advantage of providing real-time data since the leaf-morphological CO_2 signature becomes permanently fixed at the moment of leaf development, and is unaffected by diagenetic processes during burial.

The organic-rich sediments of the Roer oxbow lake are very rich in leaf remains. Stomatal frequency data for *Quercus robur* enabled the detection and quantification of short-term CO_2 fluctuations for the period between AD 1000 and 1500 (Wagner et al., 2004; van Hoof et al., 2005). Despite differences in the amplitude of the fluctuations, it could be demonstrated that, for this particular time interval, leaf-based and ice-based data sets are largely compatible (van Hoof et al., 2005). In this study, the comparison of the palynological data with the CO_2 record derived from the analysis of leaf remains from the same core provides the opportunity of a direct temporal correlation of CO_2 fluctuations and land-cover changes that could reflect Rudimann's (2003) postulated effects of the Black Death on atmospheric CO_2.

2. Study area

The studied site is an oxbow lake of the river Roer, in the vicinity of the village of Sint Odiliënberg (Province of Limburg, southeastern Netherlands, 51.08° N 6.00° E; Fig. 1). The site lies within the flooding regime of the Roer; it is repeatedly flooded especially during winter months. This part of the Netherlands belongs to the "dekzand" (cover-sand) area north of the loess district; floodplains are covered by loam, sand and gravel deposits formed by the meandering rivers, while clayey gyttja and peat deposits fill in the oxbow lakes (Berendse, 1997).

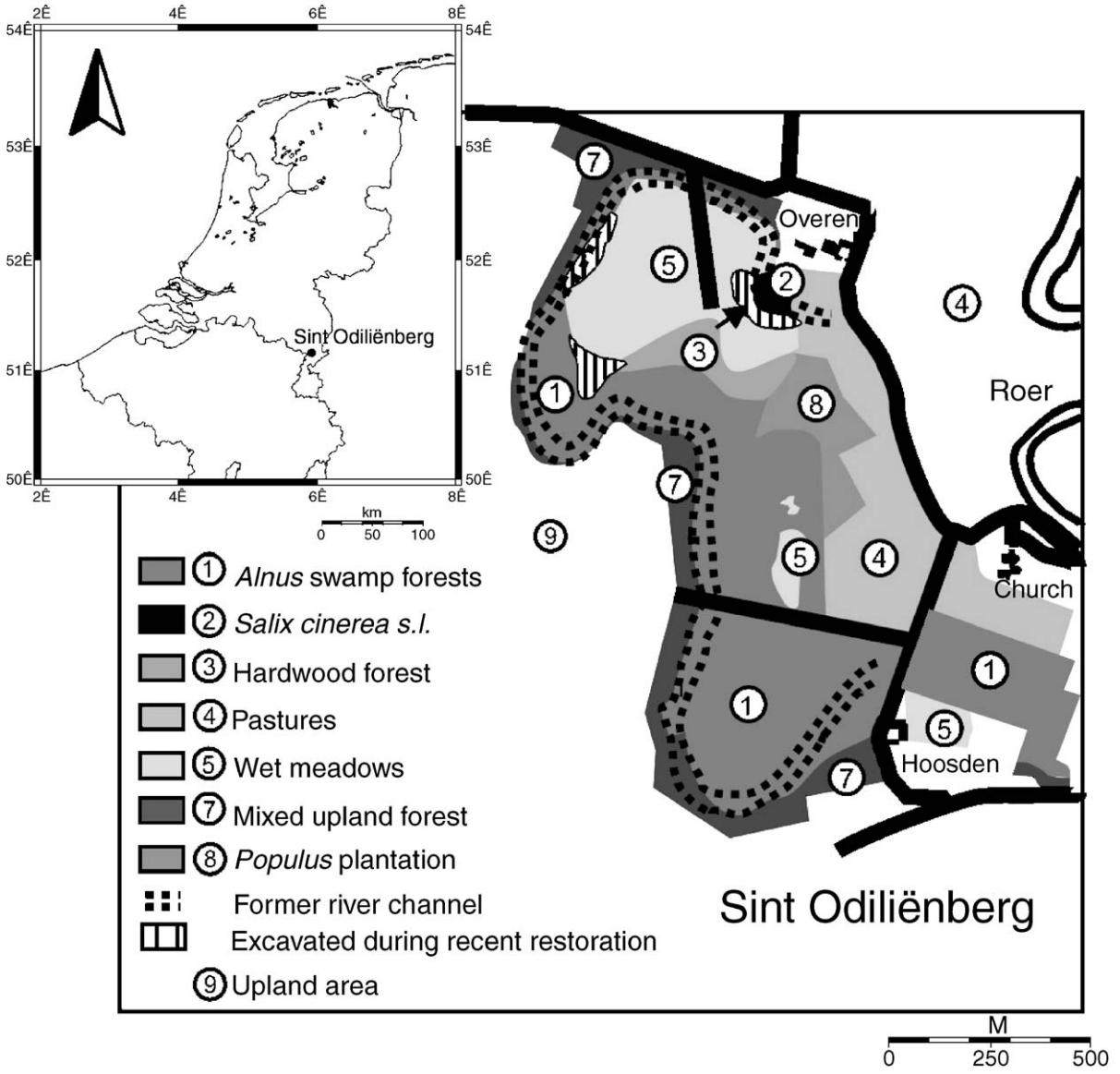

Fig. 1. Location of the studied site and local vegetation.

The coring site is located close to the church-hill of Sint Odiliënberg, which has a long history of human occupation. Parts of a Roman temple from the 4th or 5th century are still incorporated in the present church building (Willemsen, 1889; Coenen, 1922). A monastery founded in AD 700 was given to the Chapter of Utrecht in AD 858 as a refuge from Norse invaders, who eventually reached the area in AD 881. Local sources document a civil war in the area around AD 1360 resulting in the looting and burning down of several buildings in Sint Odiliënberg (Coenen, 1922; Timmermans, 1955); in AD 1361 the Chapter of Utrecht left the church-hill. In AD 1480 a new monastery was founded (Willemsen, 1889). South of the site is the Hoosden estate. It is first mentioned in historical archives around AD 1537, but its foundation may have been earlier. The continual human settlement during the studied time interval suggests a high level of human impact on the vegetation composition, which is likely to be reflected in regional and local pollen assemblages.

2.1. Natural vegetation

Without the impact of humans, the potential natural vegetation of the area would consist of deciduous forests. Mixed *Quercus–Fagus* forests with *Carpinus*, *Tilia* and *Corylus* would dominate the uplands. On the driest, nutrient-poorest, sandy soils, *Betula* would

play an important role in mixed *Quercus–Betula* forests. Those parts of the floodplains of the meandering Meuse and Roer rivers that are flooded yearly and have a year-round high groundwater table, would be covered with *Alnus–Salix–Populus* woodland (softwood gallery forest). On higher, only briefly inundated parts, the floodplains would support ALNO-PADION communities dominated by *Alnus*, *Ulmus*, *Quercus* and *Fraxinus*. In the abandoned channels, *Alnus* swamp forest (ALNION community) would replace water-plant and reed communities (after Scahaminée et al., 1998; Stortelder et al., 1998).

2.2. Present-day vegetation

Present-day vegetation on and around the site consists of *Alnus* swamp forests (Fig. 1). The wettest parts of the former oxbow lake (the coring site) are covered by *Salix cinerea s.l.* Pastures and wet meadows occupy the majority of the flood plains. On the flood plain in the vicinity of the coring site, remnants of hardwood forests (dominated by *Quercus*, *Fraxinus* and *Alnus*) and a small *Populus* plantation are present. On the steep slopes at the west bank of the meander, *Quercus* (*Q. rubra, Q. robur, Q. petraea*), *Fagus*, *Carpinus*, *Corylus* and *Betula* are the major constituents of the mixed upland forest. The upland area consists of scattered *Pinus sylvestris* and *Picea abies* plantations and arable fields, replacing larger parts of the former heath land (after Hommel and Hermans, 1996; Hermans and Peters, 1999).

3. Material and methods

A sediment core was taken in a former river channel (Fig. 1), which is completely filled with organic-rich clayey gyttja deposits and covered at the top by a peat layer. From this locality 4 m of partly laminated organic-rich sediments were recovered using a Livingstone piston corer and covered the whole channel-fill. Sediments contain abundant macrofossil remains of leaves of *Q. robur*, *Quercus petraea* and *S. cinerea s.l.* The core was cut into 0.5 cm slices, while a correction for the core compression (<5%) was applied to calculate the actual depth for each sample.

Total organic matter (TOC) was based on loss-on-ignition (LOI) measurements of the core section followed a modification of the procedure described by Dean (1974). Volume of wet material was taken from each contiguous core slice (0.5 cm) and put in a pre-weighed ceramic crucible and dried in an oven at 110 °C for 1 h, which gives the dry weight of the sample. The dried samples were then put in a muffle furnace for 1 day at 550 °C in order to remove all organic carbon. The percentage of weight loss between the dried and the ignited sample therefore represents the percentage of organic carbon that a sample contains.

Eleven samples were used for AMS ^{14}C dating at the AMS facility of the R.J. van de Graaff Laboratory (Utrecht University). All samples (Table 1) consisted of thoroughly cleaned plant macrofossil remains. Conversion of the ^{14}C dates into calendar ages AD with a 1 sigma probability has been performed with the calibration program CALIB 4.4 (Stuiver et al., 1998; Fig. 2). In order to lower uncertainty levels, the ^{14}C dates were wiggle-matched to the INTCAL98 ^{14}C calibration curve (Stuiver et al., 1998).

Pollen and spore assemblages were recovered from 0.5 cm samples with an average interval of 5 cm, following standard palynological peat-processing techniques now in use at the Laboratory of Palaeobotany and Palynology (Utrecht University; Faegri et al., 1989). Processing included carbonate and silicate removal with HCl and HF, sieving over 7 and 120 μm sieving cloth to remove fine and coarse fractions, respectively, boiling in KOH (10 min) to remove organic fractions, and acetolysis for removal of carbohydrates and coloring the pollen. The residue was mounted on microscopic slides using silicon oil. To enable calculation of pollen concentrations, tablets with a known amount of *Lycopodium* spores were added prior to processing.

For stomatal frequency analysis (van Hoof, 2004; van Hoof et al., 2005), 60 horizons of the core were sampled for leaf remains of *Q. robur*. CO_2 levels were reconstructed by using the inverse relationship between CO_2 mixing ratio (ppmv) and the area-independent stomatal index (SI=[stomatal density/(stomatal densi-

Table 1
Radiocarbon AMS ^{14}C dating results given in years BP (1950) with a 1 sigma confidence interval

Depth	Composition	^{14}C age (BP ± 1 sigma)	UTC no.
76.25	*Salix* twigs	351 ± 40	11,730
94.54	*Salix* and *Quercus* leaves	355 ± 45	12,058
111.25	*Salix* and *Quercus* leaves	369 ± 41	11,731
141.25	*Salix* and *Quercus* leaves	454 ± 37	11,732
174.84	*Salix* and *Quercus* leaves	713 ± 32	12,111
197.25	*Salix* and *Quercus* leaves	544 ± 47	11,736
210.79	*Salix* and *Quercus* leaves	783 ± 35	12,060
230.13	*Salix* and *Quercus* leaves	861 ± 30	12,059
276.4	*Salix* and *Quercus* leaves	1003 ± 39	11,733
315.8	*Salix* and *Quercus* leaves	961 ± 36	11,734
368.85	*Salix* and *Quercus* leaves	985 ± 36	11,735

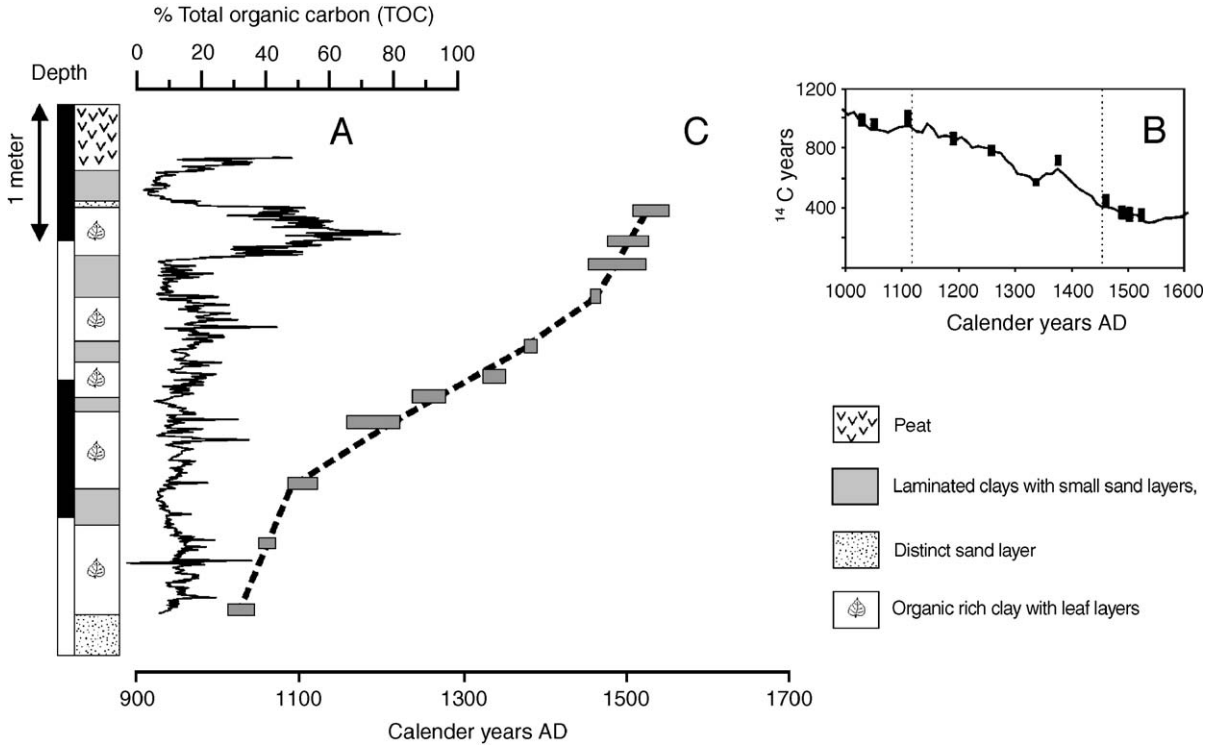

Fig. 2. A: Total organic carbon (TOC) estimates based on loss on ignition (LOI). B: Radiocarbon versus calender ages of eleven AMS ^{14}C measurements (1 sigma probability) divided in three sub-sets (dotted lines) and wiggle-matched to the INTCAL 98 calibration curve of Stuiver et al. (1998). C: Age-depth model based on the wiggle-matched ^{14}C measurements.

ty + epidermal cell density)] × 100), as monitored and modeled for this species for the atmospheric CO_2 increase of the last two centuries (van Hoof et al., in press).

4. Results

4.1. Lithology and chronology

LOI values of successive core samples fluctuate between 5% and 80% (Fig. 2A). Grey bands in the lithological column mark intervals wherein LOI remains low and relatively stable. The top of the studied core section is characterized by very high LOI values, which correspond to the presence of abundant macrofossil remains. The decrease in organic content at a depth of 75 cm corresponded with a distinctive sandy interval marking a hiatus in the sedimentary record.

Results of the AMS ^{14}C measurements are presented in Table 1. The calibration with CALIB 4.4 provides an age-depth relationship with uncertainty levels of 100–200 years. In order to lower these uncertainties, the ^{14}C dates were wiggle-matched to the INTCAL98 ^{14}C calibration curve (Stuiver et al., 1998; Fig. 2B, C). Non-wiggle-matched dates indicate that sedimentation rates are not constant throughout the core. Three periods in the depositional history could be recognized (368–276, 276–141 and 111–76 cm). Therefore the wiggle-match was performed with three different sub-sets, of which each sedimentation rate was assumed to be linear. Results of wiggle-matching are shown in Fig. 2B. The lower part (368–276 cm (1007–1100 AD)) and the upper part (111–76 cm (1463–1523 AD)) of the core section show significant higher sedimentation rates (1.17 and 1.04 cm/year, respectively), compared to the middle part (276–111 cm (1100–1463 AD); 0.29 cm/year). The wiggle-matched dates provide an age-depth model for the period of AD 1000–1500, which consists of three linear components (Fig. 2C).

Separated by a hiatus, the clays and peat deposits of the top 75 cm of the core section were formed after AD 1800 (unpublished palynological and agricultural data).

4.2. Pollen diagrams

Pollen percentage diagrams are presented in Figs. 3 and 4. Based on the age-depth model of Fig. 2, diagrams represent the regional and local vegetation development between AD 1000 and 1500. The total

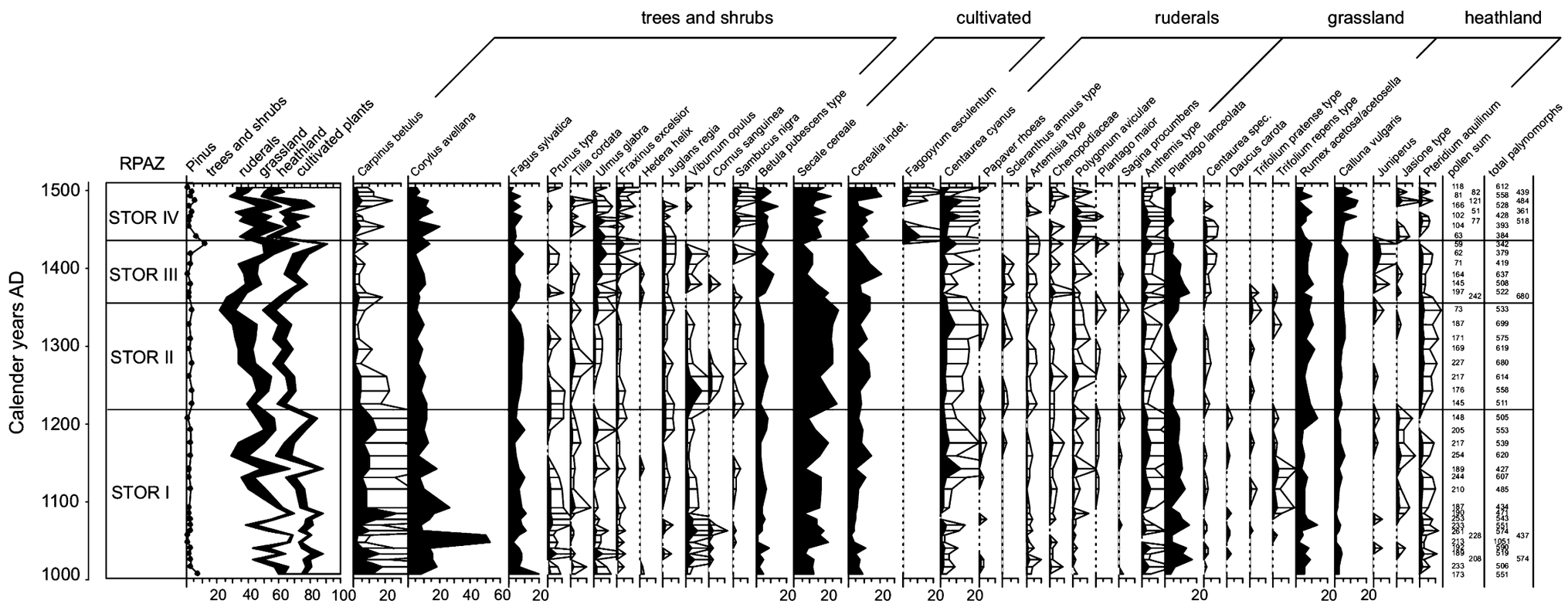

Fig. 3. Regional pollen percentage diagram.

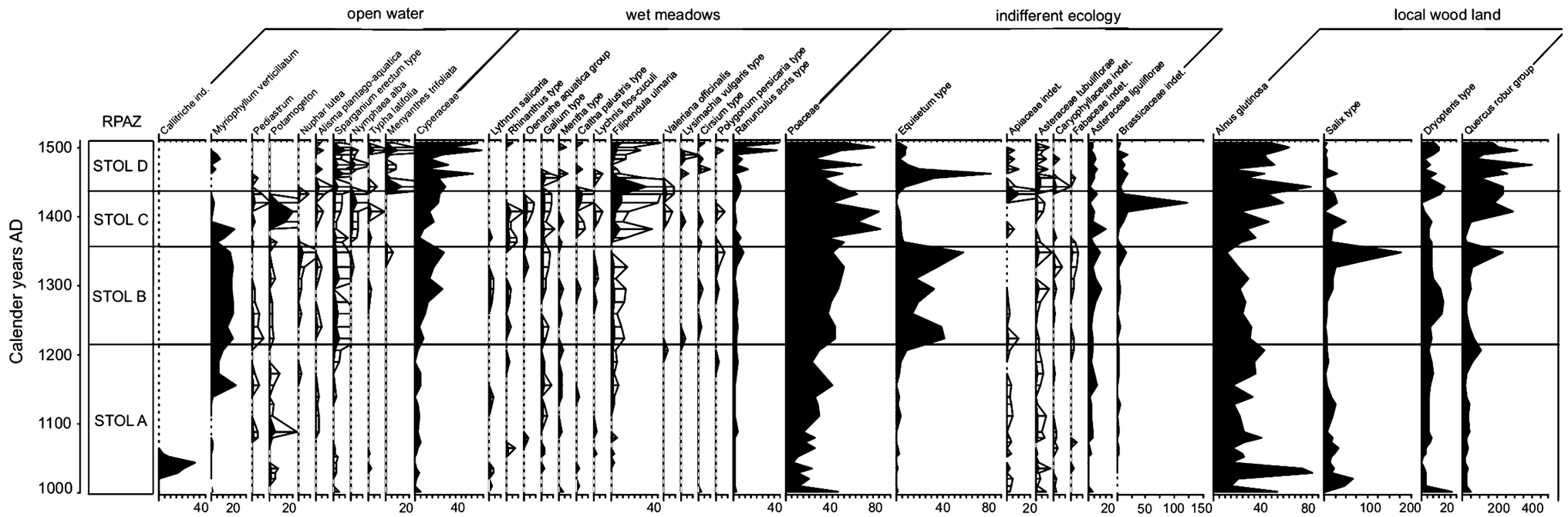

Fig. 4. Local pollen percentage diagram.

pollen assemblage consists of 148 different pollen types, of which 36 regional types and 36 local types selected types have been selected for representation in the diagrams. Concentration diagrams were calculated but not applied because of large-scale fluctuations in pollen concentrations, probably resulting from the presence of abundant macrofossil remains in the palynological samples.

The pollen sum, the calculation base for both regional and local pollen percentages, consists of pollen types from upland plants. In the regional pollen diagram (Fig. 3) these are represented by five ecological groups: pollen from (1) trees and shrubs, (2) cultivated plants, (3) ruderals, (4) grassland, and (5) heathland. The cumulative curves of these five pollen groups are displayed in panels at the left side of the individual regional pollen curves. The pollen record of *Pinus* is presented as an overlay curve.

Pollen of *Alnus* and *Salix* are excluded from the pollen sum because both taxa are locally growing at the coring site. Also oak pollen (*Q. robur* group) is excluded. The sediments contain numerous macrofossil remains (leaves), and the finding of sub-fossil *Q. robur* trunks, 9 m from the coring site, confirms the local presence of full-grown oak trees from AD 1330 to 1550 (van Hoof, 2004). Also the dominance of oak pollen during several intervals, makes it clear that *Quercus* had to be treated as an (extra-) local constituent of the vegetation (sensu Janssen, 1973).

The group "cultivated plants" contains pollen of cereals (Cerealia indet., *Secale cereale* and *Fagopyrum esculentum*). The group "ruderals" includes pollen types of arable weeds and plants from other ruderal plant communities. The "grassland" group comprises pollen types of drier meadows and pastures. Since the *Anthemis* pollen type is produced by plants common in ruderal communities (*Anthemis* spp., *Matricaria* spp., *Tanacetum vulgare*), as well as by grassland plants (*Achillea millefolium*, *Leucanthemum vulgare*), this pollen represents both groups.

Poaceae pollen is excluded from the pollen sum, since *Phragmites* (reed) is present in both the potential and the present vegetation of the coring site. The group "heathland" represents pollen (and spores) of heather communities (*Calluna vulgaris*) and of plants growing on acid, nutrient-poor soils such as *Juniperus* and *Pteridium aquilinum*. Due to poor preservation of the material, no discrimination of *Rumex acetosella* (a species indicative of acid sandy soils) and *R. acetosa* (a meadow species) has been attempted, the recognized pollen type *R. acetosa*/*acetosella* is regarded to represent both grassland and heathland.

The local pollen diagram (Fig. 4) comprises four ecological groups: (1) pollen of plants from open water, (2) pollen from wet meadows (communities influenced by groundwater), (3) pollen (and spores) of taxa with no distinct ecological preference, such as Poaceae, Asteraceae and *Equisetum*, and pollen of local tree species (*Alnus glutinosa*, *Salix* type, *Q. robur* group).

4.3. Pollen assemblage zones

Distinct changes in the composition of both regional and local pollen assemblages allow the recognition of four regional pollen assemblage zones (STOR I–IV) and four local pollen assemblage zones (STOL A–D):

STOR I (368–222 cm; AD 1007–1220). In this zone, pollen of *Carpinus betulus, Corylus avellana* and *Fagus sylvatica* dominates the arboreal pollen (total AP ca. 50%). In addition, pollen from grassland elements and cereals (Cerealia indet., *S. cereale*) plays an important role. The upper zonal boundary (ca. AD 1220) is marked by a distinctive decline of the *Carpinus* curve and by increasing values for cereal pollen, particularly *S. cereale*.

STOR II (222–186 cm; AD 1220–1350). This zone is characterized by a steady increase of non-arboreal pollen (NAP). *S. cereale* reaches maximum values of 25% towards the top of the zone. Decreasing values for *S. cereale*, *Centaurea cyanus* and spores of *P. aquilinum* mark the upper boundary the zone (ca. AD 1350).

STOR III (186–153 cm; AD 1350–1430). This zone displays a continuing decrease of total NAP pollen. Notably the *S. cereale* curve shows a distinctive decline, reaching minimum values of 5% at the top of the zone. Values of *Ulmus glabra* type, *Fraxinus excelsior* and *Juniperus* cause a concomitant AP increase. A distinct *Pinus* peak occurs at the top of the zone. Grassland pollen types show high values of *Plantago lanceolata* at the base of the zone. The upper boundary (ca. AD 1430) is defined by renewed increase of *S. cereale* and the first occurrence of pollen of *F. esculentum*.

STOR IV (153–76 cm; AD 1430–1553). This zone is characterized by high NAP values, particularly cereals, and by the presence of *Fagopyrum* pollen. The *Pinus* curve drops back to values <5%, *Juniperus* pollen is absent.

STOL A (368–222 cm; AD 1007–1220). The local assemblage is dominated by pollen of *A. glutinosa*, Poaceae and, especially in the basal part of the zone,

by *Salix* type pollen. The open water plants are represented by a brief increase of *Callitriche*, by *Potamogeton* and, in the upper part of the zone, by the pollen of *Myriophyllum verticillatum*. The upper zonal boundary (ca. AD 1210) is placed at the rise of the curves for Cyperaceae, Poaceae and *Filipendula*, a sharp increase of *Equisetum* type spores, and the decline of *A. glutinosa* and *Quercus*.

STOL B (222–186 cm; AD 1220–1350). This zone is characterized by high values of *M. verticillatum*, *Sparganium erectum* type, Cyperaceae and *Equisetum* type spores. The curves for *Quercus* and *Salix* show peak values at the top of the zone (>200%), where the *Alnus* curve reaches minimum values (<20%). The upper boundary of the zone (ca. AD 1350) is marked by the drop of *Equisetum*, *Salix* and *Quercus*.

STOL C (186–153 cm; AD 1350–1430). In this zone maximum values for Poaceae; *Filipendula*, and Cyperaceae are reached, while *Alnus* values increase. Relatively high values of *Nymphaea*, *Potamogeton* and Brassicaceae indet. are also characteristic of this zone. The upper boundary (ca. AD 1430) is placed at the rise of *Equisetum, Filipendula* and *Menyanthes.*

STOL D (153–76 cm; AD 1430–1553). This zone is dominated by pollen of *Alnus*, *Quercus* and Cyperaceae. *Equisetum* type spores rise to maximum values in the lower part of the zone.

5. Vegetation development and land use AD 1000–1500

The main feature of the analyzed pollen record is a long-term reduction of the arboreal component reflecting regional deforestation up to 1350 AD, parallel to the population increase during this period (Slicher-van-Bath, 1962). The same feature is recorded in pollen diagrams from the adjacent loess area in Germany and southern Limburg (Phase G, H of Bunnik, 1999). For the whole period, the regional diagram (Fig. 3) reflects a landscape that is completely altered by intensive agricultural activities. Woodland is exceedingly transformed to arable fields, grassland (pastures and meadows) and heath land.

Cereals, notably *S. cereale,* were the most prominent crop, even on nutrient-poor soils. The relatively high pollen values for the accompanying weed *C. cyanus* indicate that cereals were commonly grown as winter cereals. In the agricultural system, heathland was the main production area of sheep and cattle dung. High values of *C. vulgaris* underline the increasing importance of heathland in the 15th century. This agrees well with historical records from southern Limburg, where heathland reached its greatest expansion at the end of the medieval period (Hillegers, 1980). The introduction of *F. esculentum* (buckwheat), which is tolerant of low-nutrient conditions, around AD 1450 (Zone STOR IV) can be regarded as an adaptation to the increasing nutrient deficiency of the sandy soils after centuries of agricultural use. Historical records show that buckwheat cultivation in The Netherlands started at the end of the 14th century; the low-nutrient demanding crop became increasingly important in the course of the following centuries (Leenders, 1987).

The local vegetation development reflects an infilling and terrestrialization process (Fig. 4). In the basal part of Zone STOL A, early successional open-water vegetation of the oxbow is represented by a short-lived peak of *Callitriche*, probably *C. platycarpa*, a species that is often the only water plant in flowing waters. In the succeeding slow-flowing and stagnant phases, this element was rapidly outcompeted by other open-water plants, such as *M. verticillatum*, *Potamogeton*, *Nuphar lutea* and *Nymphaea alba*. Also the curve for *Equisetum* spores may indicate terrestrialization. The species involved is most likely *E. fluviatile*, a pioneer plant in calm shallow waters. In the lateral and succeeding reed vegetation, Cyperaceae and probably also Poaceae (*Phragmites*) played the dominant role, while *S. erectum* and *Typha latifolia* were common elements.

5.1. Agricultural crises and associated periods of reforestation

Apart from some earlier short-lived fluctuations, the regional pollen diagram shows a distinctive low in cereal pollen in upper part of Zone STOR I. The anomaly covers a few decades (ca. AD 1180–1215), and may reflect an agricultural crisis caused by consecutive crop failures. This crisis had considerable impact on the landscape. Decline of cereal pollen is accompanied by low values of *C. vulgaris* and an increase in tree pollen (*Carpinus*, *Betula*, *Ulmus*, *Quercus*).

In The Netherlands and large parts of northwestern Europe, the last quarter of the 12th century and the 13th century is characterized by a shift from a relatively stable climate, the so-called Medieval Climatic Optimum (or Medieval Warm Period), to more extreme climate oscillations (Lamb, 1977; Buisman, 1995; Fagan, 2000). The shift may be regarded as the transition to the Little Ice Age, a lengthy unstable period that lasted until the 19th century when the current period of global warming began. Although in northwestern Europe this

period started with warm, extremely wet winter conditions that lasted until AD 1430 (Buisman, 1995; Fagan, 2000), the main long-term feature of the Little Ice Age climate oscillations was a declining temperature trend combined with low average-temperature anomalies (Lamb, 1977).

By the end of the 12th century, average weather conditions were no longer optimal for agriculture. In various parts of western Europe, historical sources record a famine in AD 1196 caused by several years of crop failure due to wet conditions during harvest season (Buisman, 1995). Also in Cologne, the largest medieval city in the vicinity of the studied area, there was a great shortage of cereals and other food supplies. Reduced tilling resulted in woodland regeneration on previously farmed land. Evidenced by a strong increase of *S. cereale* pollen, full recovery of agriculture took place after AD 1215 (base Zone STOR II).

Following the period with maximum values for non-arboreal pollen at the top of Zone STOR II, a period of prolonged and pronounced agricultural regression can be identified in the regional pollen record of Zone STOR III (ca. AD 1360–1440). At first, the curves for *S. cereale* and *C. cyanus* drop sharply. At the same time, *P. lanceolata* reaches high values. Subsequent features are increasing percentages of *Betula* pollen, followed by increasing values for *Ulmus*, *Fraxinus* and *Juniperus*-type, while the curve for *P. lanceolata* drops concomitantly. At the end of the zone, *Pinus* and *Juniperus*-type reach maximum values.

The pollen record of Zone STOR III can be interpreted as a strong reduction of cereal production. The sharp increase in *P. lanceolata*, accompanied by increasing local values for Poaceae in Zone STOL C may point to a conversion of cereal fields into grassland, but could also be interpreted as an initial step in a natural vegetation succession on fallow land (Behre, 1981). Subsequent decline of *P. lanceolata*, increasing values of *Ulmus* and *Fraxinus*, together with increasing local values for *Alnus* and *Quercus* in Zone STOL C, indicate growth and expansion of hardwood floodplain forests (ALNO-PADION communities) on rich loamy soils, at the expense of meadows and pastures. High percentages of *Pinus* and *Juniperus*-type pollen in the uppermost part of Zone STOR III are indicative for a reforestation succession on poor sandy soils.

Progressively increasing percentages of *Filipendula ulmaria* in Zone STOL C suggest the reduction of mowing and grazing pressure on wet floodplain meadows in the vicinity of the coring site. Because it is flowering in mid-summer, this grassland species is strongly suppressed by mowing and grazing. When these agricultural activities are discontinued, wet meadows may convert into tall forb communities where *F. ulmaria* finds optimal growing conditions. Cessation of mowing and grazing could well be ascribed to the regional agricultural crisis. An alternative, natural cause for the abandonment of wet meadows could be the excessive 14th-century AD winter precipitation in The Netherlands (Buisman, 1995), resulting in meadows that were too wet for cattle to graze on.

Decreasing trends in the frequency of cereal pollen during the 14th and 15th centuries have long since been recorded in pollen diagrams from various parts of western Europe (Overbeck and Griez, 1954; Phillippi, 1965; Wiethold, 1998; Bunnik, 1999). This long-term decrease has been linked to a prolonged period of agricultural crisis that had started already at the beginning of the 14th century (Slicher-van-Bath, 1962). Agricultural decline is also evident from historical sources that record large-scale desertion of farms and rural villages in Europe ('lost villages' in England; 'Wüstungen' in Germany) (Bieleman, 1992). A prolonged late medieval crisis is primarily considered to be a response to the effects of unstable climatic conditions in combination with the increasing population density in western Europe. Frequent failure of harvest is held responsible for a gradual weakening of both population and economy. Malnutrition could then have paved the way for epidemic outbreaks of plague and other diseases, culminating in the spread of the Black Death, which decimated the population of large parts of Europe (Slicher-van-Bath, 1962; Cartwright, 1972; Lamb, 1977; Fagan, 2000). Recent research questions the presence of a significant agricultural crisis *before* the spread of the Black Death (e.g. Janssen, 1997; Stebich et al., 2005). Despite occasional famine, in the first half of the 14th century the European population continued to grow, with a concomitant overall increase of agricultural activity (Janssen, 1997).

Also in the study area, there is no evidence of agricultural crisis before AD 1350. With maximum values for *S. cereale* in the upper part of Zone STOR II, the pollen record demonstrates increasing rather than decreasing agricultural activity. The onset of agricultural regression at the base of Zone STOR III corresponds with regional plague outbreak given the error margin associated with the age model. The Black Death entered the border region of the southeastern Netherlands and Germany in AD 1349 (Creutz, 1933; Schmitz-Cliever, 1954). In the big cities of the region, like Cologne and Aachen, plague may have killed about one third of the populace in AD 1349–1350.

Similar to the situation in other parts of Europe (e.g. Cartwright, 1972), the impact of the Black Death on agriculture became progressively apparent in the years following the outbreak. Due to high mortality rates among rural peasants, labour had become scarce. Landlords, reluctant to pay higher wages, began to raise more cattle and sheep. Part of the farmland, particularly on nutrient-poor soils, was simply abandoned so that it could turn back into forest. The increasing number of peasant revolts in Europe, locally documented for Sint Odiliënberg (Coenen, 1922; Timmermans, 1955), may have reinforced this process of agricultural decline (Mollat and Wolf, 1973). The agricultural regression lasted about 80 years. Rapid increase of cereal pollen and the introduction of buckwheat at the transition of Zones STOR III and STOR IV confirms recovery of agriculture after AD 1440. This date is consistent with the ending of late medieval agricultural crisis recognized elsewhere in Europe (Slicher-van-Bath, 1962).

A comparable, plague-induced agricultural regression has been identified in detailed pollen records from Schleswig–Holstein, northern Germany (Wiethold, 1998). Unfortunately, however, these records are not constrained by an accurate ^{14}C time-framework. The Black Death is used as the very datum for determining the onset of agricultural decline in these records. A vegetation reconstruction based on pollen analysis from a varved sediment record from Lake Pavin in France recognized an agricultural regression accompanied by a reforestation from AD 1350 to 1475 (Stebich et al., 2005). These results are comparable to those of the present study with respect to timing, nature and duration of this event.

5.2. Atmospheric CO_2 during the period of forest re-growth

The recognition of regional, plague-induced regression of agriculture, as reflected in the pollen spectra of Zone STOR III, is in agreement with the concept of Rudimann (2003) that abandoned farmland could act as a significant terrestrial carbon sink. Towards the top of the zone, the contribution of cereal pollen in the assemblage is roughly halved (from ca. 40% to ca. 20%).

Forests can reclaim farmland within 50 years. The present study only identifies the timing of a regional reforestation signal and therefore provides no conclusive information about the exact size of a supposed Eurasian carbon sink. According to calculations by Rudimann (2003), 14–27 Gt of terrestrial carbon sequestration would be required to explain CO_2 anomalies in the range of 4–10 ppmv recorded in Antarctic ice cores. At the time of the Black Death and its aftermath, reforestation at a level of 25% to 45% of the total arable area of Europe and Asia could account for this amount (Rudimann, 2003). Although quantitative trends in the composition of regional pollen spectra may be influenced by factors other than changes in the size of farmed land, the strongly reduced contribution of cereal pollen of Zone STOR III could well comply with such figures. It is questionable, however, whether the Black Death provided comparable preconditions for reforestation throughout Eurasia. Recent historical research suggests that the geographical spread of the plague in Europe was less extensive than previously thought (Vasold, 2003). Moreover, there is no compelling evidence of widespread coeval plague outbreak in Asia.

Rudimann's (2003) proposal that the Black Death and its aftermath could have been responsible for a CO_2 drop of 4–10 ppmv is based mainly on the presumed CO_2 anomaly measured in the ice cores of Taylor Dome between AD 1300 and 1400 (Indermühle et al., 1999). However, data from different Antarctic coring localities are not in agreement with respect to timing and magnitude of CO_2 changes during the past millennium. The ice-core record from Law Dome suggests that a prominent negative anomaly occurred later, between AD 1600 and 1800 (Etheridge et al., 1996), while ice cores from South Pole and Adélie Land (D47) register negative anomalies around AD 1200 and AD 1450 (Siegenthaler et al., 1988; Barnola et al., 1995). The most recent Antarctic CO_2 record from Dronning Maud Land (Siegenthaler et al., 2005) does not reveal a CO_2 anomaly, which could be linked to the Black Death pandemic.

It should be noted that effects of natural gas diffusion processes in the firn are inherent to ice-core records (e.g. Trudinger et al., 2003). Next to a smoothing of the amplitude of the CO_2 signal, diffusion is responsible for a gas–ice age difference in ice cores, resulting in considerable age-uncertainties for CO_2 records of the last millennium (e.g. for ~100 years for Taylor Dome (Indermühle et al., 1999)). These effects hamper the accurate temporal correlation of ice-derived CO_2 fluctuations and records of plague-induced forest re-growth.

In contrast to ice-core records, the CO_2 reconstruction based on stomatal frequency analysis of *Q. robur* leaf remains from the investigated site (Fig. 5B) provides the opportunity of a direct temporal correlation of the recorded changes in land-cover following the Black Death pandemic and changes in atmospheric CO_2, without the bias naturally incorporated in age models. A comparative study demonstrated that fluctuations in

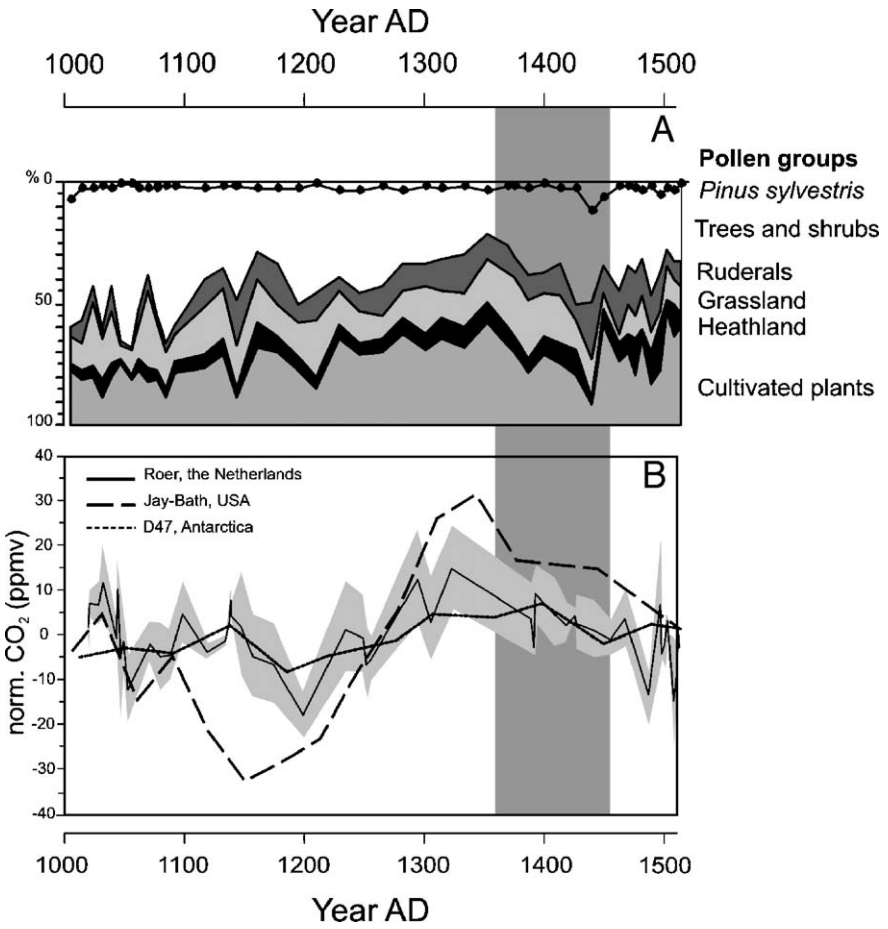

Fig. 5. A: Summary diagram of the regional vegetation development based on pollen analysis (see also Fig. 3). The grey area marks the zone interpreted to reflect forest re-growth on the abandoned farmlands after the Black Death. B: Three different atmospheric CO_2 records. Two are based on stomatal frequency analysis (thin black line with grey error envelope: Sint Odiliënberg, The Netherlands: van Hoof, 2004; van Hoof et al., 2005 and striped line: Jay-Bath, USA: Kouwenberg et al., 2005) of which one (Sint Odiliënberg) is based on *Q. robur* leaves derived from the same sediment core as the palynological based vegetation reconstruction of Fig. 5A. The third record (solid black line) is an alternative Antarctic ice-core record from Adelié Land (Barnola et al., 1995).

the leaf-based CO_2 reconstruction are similar to CO_2 trends based on records of conifer needles from Mount Rainier, Washington, USA (Wagner et al., 2004; Kouwenberg et al., 2005; van Hoof et al., 2005; Fig. 5B). Differences in the amplitude of the fluctuations are likely to be related to remaining uncertainties in the newly developed inference models for conifers (Kouwenberg et al., 2003; Wagner et al., 2004). There are also similarities in timing and duration with CO_2 fluctuations recognized in coeval Antarctic ice-core records from the South Pole and D47 sites (Siegenthaler et al., 1988; Barnola et al., 1995). Results of the two independent methods differ significantly in the amplitude of the reconstructed CO_2 fluctuations (10 ppmv ice-core, versus 34 ppmv stomatal frequency). However, by using a firn diffusion model, such discrepancies could be well explained as an effect of smoothing resulting from gas diffusion in the firn layer at the site of the ice cores. The discrepancies strongly diminish when the raw stomatal frequency data are smoothed analogously to the natural smoothing which occurs in the firn (van Hoof et al., 2005; Fig. 5B).

There is a remarkable correspondence between CO_2 trends of the 13th–15th centuries and coeval trends in regional forest density as reflected in the pollen record (Fig. 5). Regardless of differences in amplitude, both leaf-based and compatible ice-based records reflect a pronounced CO_2 minimum around AD 1200, followed by an increase during the 13th century. This increase could well correspond to large-scale forest clearance in Europe (Williams, 2003). During the period of maximum reforestation between AD 1400 and 1440, CO_2 levels seem to be relatively low. Unfortunately, the precise timing of the onset of a CO_2 decline is difficult

to assess on the basis of the data so far available. A long-term declining trend may have started already before the spread of the Black Death in Europe, and seems to continue after the ending of late medieval agricultural crisis around AD 1450.

6. Conclusions

Palynological information from the southeastern part of The Netherlands allows, for the first time, a relatively clear reconstruction of the nature and precise timing of regional effects of the mid-14th century Black Death on late medieval agriculture crisis. The pollen record reflects significant agricultural regression accompanied with forest re-growth on the deserted farmlands at the time of the Black Death and its aftermath (AD 1350–1440).

Although the pollen record confirms Rudimann's (2003) concept that plague-induced reforestation of abandoned farmland could promote terrestrial carbon sequestration, direct temporal correlation with proxy CO_2 records based on stomatal frequency analysis does not unequivocally corroborates his hypothesis of a specific role of the Black Death in short-term atmospheric CO_2 dynamics of the last millennium. However, considering the apparent correspondence between forest density changes and CO_2 trends of the 13th–15th centuries, plague-induced carbon sequestration in Europe could have contributed to a longer-term process of CO_2 decline that had already started before the spread of Black Death in Europe.

Acknowledgements

We would like to thank A.F. Lotter, F. Wagner, T.H. Donders and two anonymous reviewers for constructive comments on the manuscript. K. van der Borg is thanked for his help with the AMS ^{14}C dating. This project was financially supported by NWO (Netherlands Organisation for Scientific Research; project number: 83523002). This is NSG publication number 20051202.

References

Barnola, J.M., Anklin, M., Porcheron, J., Raynaud, D., Schwander, J., Stauffer, B., 1995. CO_2 evolution during the last millennium as recorded by Antarctic and Greenland ice. Tellus 47B, 264–272.

Behre, K.E., 1981. The interpretation of anthropogenic indicators in pollen diagrams. Pollen et Spores 23, 225–245.

Berendse, H., 1997. Landschappelijk Nederland. Fysische geografie van Nederland. van Gorcum, Assen.

Bieleman, J., 1992. Geschiedenis van de landbouw in Nederland 1500–1950. Boom Meppel, Amsterdam.

Bray, R.S., 1996. Armies of Pestilence. The Lutterworth press, Cambridge.

Buisman, J., 1995. Duizend jaar weer, wind en water in de lage landen. van Wijnen, Franeker.

Bunnik, F.P.M., 1999. Vegetationsgeschichte der LöBbörden zwischen Rhein und Maas-von der Bronzezeit bis in die frühe Neuzeit. P.h.D. thesis, Laboratory of Palaeobotany and Palynology, Utrecht University, Utrecht, 1–149 pp.

Cartwright, F.F., 1972. Disease and History. Northumberland Press Limited, Gateshead.

Caspersen, J.P., Pacala, P.W., Jenkins, J.C., Hurtt, G.C., Moorcroft, P.R., Birdsey, R.A., 2000. Contributions of land-use history to carbon accumulation in U.S. forests. Science 290, 1148–1150.

Coenen, J., 1922. De drie munsters der Maasgouw, Aldeneyck, Susteren, St.-Odiliënberg. Publications de la Société Historique et Archéologique dans le limburg.

Creutz, R., 1933. Pest und Pestabwehr im alten Köln. Jahrbuch des Kölner Geschichtsvereins 15, 79.

Dean, W.E., 1974. Determination of carbonate and organic matter in calcareous sediments and sedimentary rocks by loss on ignition: a comparison with other methods. Journal of Sedimentary Petrology 44, 249–253.

Dixon, R.K., Brown, S., Houghton, R.A., Solomon, A.M., Trexler, M.C., Wisniewski, I., 1994. Carbon pools and flux of global forest ecosystems. Science 263 (5144), 185–190.

Etheridge, D.M., Steele, L.P., Langenfels, R.L., Francey, R.J., Barnola, J.M., Morgan, V.I., 1996. Natural and anthropogenic changes in atmospheric CO_2 over the last 1000 years from air in Antarctic ice and firn. Journal of Geophysical Research 101 (D2), 4115–4128.

Faegri, K., Kaland, P.E., Krzwinsky, K., 1989. Text Book of Pollen Analysis. John Wiley and Sons, Chichester.

Fagan, B., 2000. The Little Ice Age: How Climate Made History. Basic Books, New York.

Hermans, J.T., Peters, G.M.T., 1999. Flora en vegetatie van landgoed Hoosden, Stichting de Lierelei.

Hillegers, H.P.M., 1980. Heidevelden in het Mergelland. Natuurhistorisch Maandblad 67, 121–141.

Hommel, P.W.F.M., Hermans, J.T., 1996. Het Landgoed Hoosden en de Turfkoelen. In: Hommel, P.W.F.M., Horsthuis, M.A.P. (Eds.), Excursieverslagen Van De Plantensociologische Kring Nederland.

Houghton, R.A., Skole, D.L., 1990. Carbon. In: Turner, B.L., et al., (Eds.), The Earth as Transformed by Human Action. Cambridge University Press, Cambridge.

House, J.I., Prentice, C., LeQuere, C., 2002. Maximum impacts of future reforestation or deforestation on atmospheric CO_2. Global Change Biology 8, 1047–1052.

Indermühle, A., et al., 1999. Holocene carbon-cycle dynamics based on CO_2 trapped in ice at Taylor Dome, Antarctica. Nature 398, 121–126.

Janssen, C.R., 1973. Local and regional pollen deposition. In: Birks, H.J.B., West, R.G. (Eds.), Quartenary Plant Ecology, 14th Symposium of the British Ecological Society, pp. 31–42.

Janssen, W., 1997. Kleine Rheinische Geschichte. Patmos Verlag, Düsseldorf.

Jessen, C.A., Rundgren, M., Björck, S., Hammerlund, D., 2005. Abrupt climatic changes and an unstable transition into a late Holocene thermal decline: a multiproxy lacustrine record from southern Sweden. Journal of Quartenary Science 20 (4), 349–362.

Kouwenberg, L.L.R., McElwain, J.C., Kürschner, W.M, Wagner, F., Beerling, D.J., Visscher, H., 2003. Stomatal frequency adjustment

of four conifer species to historical changes in atmospheric CO_2. American Journal of Botany 90, 610–619.

Kouwenberg, L.L.R., Wagner, F., Kürschner, W.M., Visscher, H., 2005. Atmospheric CO_2 fluctuations during the last millennium reconstructed by stomatal frequency analysis of *Tsuga heterophylla* needles. Geology 33 (1), 33–36.

Kürschner, W.M., 1996. Leaf stomata as biosensors of palaeoatmospheric CO_2 levels. LPP Contributions Series 5. P.h.D. thesis, Utrecht University.

Lamb, H.H., 1977. Climatic History and the Future. Climate: Present, Past and Future. Methuen & co Ltd, London.

Leenders, K.A.H.W., 1987. De boekweitkultuur in historisch perspectief. Geologisch Tijdschrift 21, 213–227.

McElwain, J.C., Mayle, F.E., Beerling, D.J., 2002. Stomatal evidence for a decline in the atmospheric CO_2 concentration during the Younger Dryas stadial: a comparison with Antarctic ice core records. Journal of Quartenary Sciences 17, 21–29.

Mellilo, J.M., Fruci, J.R., Houghton, R.A., Moore, B., Skole, D.L., 1988. Land-use changes in the Sovjet Union between 1850 and 1980: cause of a net release of CO_2 to the atmosphere. Tellus 40B, 116–128.

Mollat, M., Wolf, P., 1973. The Popular Revolutions of the Late Middle Ages. George Atkin and Unwin Ltd., London.

Overbeck, F., Griez, I., 1954. Mooruntersuchungen zur Rekurrenzflächenfrage und Siedlungsgeschichte in der Rhön. Flora 141, 21–99.

Phillippi, S., 1965. Zur Datierung eines Plattenweges am Wurmberg/Oberharz mit Hilfe de Pollenanalyse, Neue Ausgrabungen und Forschungen in Niedersachsen. August Lax, Hildesheim.

Royer, D.L., 2001. Stomatal density and stomatal index as indicators of paleoatmospheric CO_2 concentration. Review of Palaeobotany and Palynology 114 (1–2), 1–28.

Rudimann, W.F., 2003. The anthropogenic greenhouse era began thousands of years ago. Climatic Change 61, 261–293.

Rundgren, M., Beerling, D.J., 1999. A Holocene CO_2 record from the stomatal index of subfossil *Salix herbacea* L. leaves from northern Sweden. Holocene 9, 509–513.

Rundgren, M., Björck, S., 2003. Late-glacial and early Holocene variations in atmosperic CO_2 concentration indicated by high-resolution stomatal index data. Earth and Planetary Science Letters 213, 191–204.

Scahaminée, J.H.J., Weeda, E.J., Westhof, V., 1998. De vegetatie van Nederland. Opulus Press, Leiden Upsala.

Schmitz-Cliever, E., 1954. Pest und pestilenzische Krankheit in der Geschichte der Reichsstadt Aachen. Zeitschrift des Aachener Geschichtsvereins 66/67, 55.

Siegenthaler, U., Friedli, H., Lötscher, H., Moor, A., Neftel, A., Oeschger, H., Stauffer, B., 1988. Stable-isotope ratio and concentration of CO_2 in air from polar ice cores. Annals of Glaciology 10, 151–156.

Siegenthaler, U., Monnin, E., Kawamura, K., Spahni, R., Schwander, J., Stauffer, B., Stocker, T.F., Barnola, J.M., Fischer, H., 2005. Supporting evidence from the EPICA Dronning Maud Land ice core for atmospheric CO_2 changes during the past millennium. Tellus 57B, 51–57.

Slicher-van-Bath, B., 1962. De agrarische geschiedenis van west-Europa (500–1850). Het Spectrum, Utrecht Antwerpen.

Stebich, M., Brüchmann, C., Kulbe, T., Negendank, J.W.F., 2005. Vegetation history, human impact and climate change during the last 700 years recorded in annually laminated sediments of Lac Pavin, France. Review of Palaeobotany and Palynology 133, 115–133.

Stortelder, A.H.F., Hommel, P.W.F.M., Waal, R.W.d., 1998. Broekbossen. Bosecosystemen van Nederland. KNNV, Utrecht.

Stuiver, M., Reimer, P.J., Bard, E., Beck, J.W., Burr, G.S., Hughen, K.A., Kromer, B., McCormac, G., van der plicht, J., Spurk, M., 1998. INTCAL98 radiocarbon age calibration, 24.000–0 cal. BP. Radiocarbon 40, 1041–1084.

Taylor, L., 1983. Everyday Life: The Seventeenth Century. Silver Burdett Company, Morristown.

Timmermans, H., 1955. St. Odiliënberg, Historische schets over het oudste pelgrimsoord van midden-Limburg, Roermond.

Trudinger, C.M., Rayner, p.J., Enting, I.G., Heimann, M., Scholtze, M., 2003. Implications of ice core smoothing for inferring CO_2 flux variability. Journal of Geophysical Research 108, 4492.

van Hoof, T.B., 2004. Coupling between atmospheric CO_2 and temperature during the onset of the Little Ice Age, LPP Contributions series No. 18, P.h.D. thesis, Utrecht University.

van Hoof, T.B., Kaspers, K.A., Wagner, F., van de Wal, R.S.W., Kürschner, W.M., Visscher, H., 2005. Atmospheric CO_2 during the 13th century AD: reconciliation of data from ice core measurements and stomatal frequency analysis. Tellus 57B, 351–355.

van Hoof, T.B., Kürschner, W.M., Wagner, F., Visscher, H., in press. Stomatal index response of *Quercus robur* and *Quercus petraea* to the anthropogenic atmospheric CO_2 increase. Plant Ecology.

Vasold, M., 2003. Die Ausbreitung des Schwarzen Todes in Deutschland nach 1348: Zugleich ein Beitrag zur deutschen Bevölkerungsgechichte. Historische Zeitschrift 277 (2), 281–308.

Wagner, F., Below, R., De Klerk, P., Dilcher, D.L., Joosten, H.J.H., Kürschner, W.M., Visscher, H., 1996. A natural experiment on plant acclimation: lifetime stomatal frequency response of an individual tree to annual atmospheric CO_2 increase. Proceedings of the National Academy of Sciences of the United States of America 93, 11705–11708.

Wagner, F., Bohncke, S.J.P., Dilcher, D.L., Kürschner, W.M., van Geel, B., Visscher, H., 1999. Century-scale shifts in early Holocene atmospheric CO_2 concentration. Science 284, 1971–1973.

Wagner, F., Aaby, B., Visscher, H., 2002. Rapid atmospheric CO_2 changes associated with the 8.200-years B.P. cooling event. Proceedings of the National Academy of Sciences 99, 12011–12014.

Wagner, F., Kouwenberg, L.L.R., van Hoof, T.B., Visscher, H., 2004. Reproducibility of Holocene atmospheric CO_2 records based on stomatal frequency. Quarternary Science Reviews 23, 1947–1954.

Wiethold, J., 1998. Studien zur jüngeren postglazialen Vegetations- und Siedlungsgeschichte im östlichen Schleswig–Holstein, P.h.D. Thesis, Universität Kiel, Kiel.

Willemsen, M.A.H., 1889. Oorkonden en bescheiden aangaande de kerk en het kapittel van Sint Odiliënberg. Heemkunde vereniging Roerstreek, Sint Odiliënberg.

Williams, M., 2003. Deforesting the Earth from Prehistory to Global Crisis. University of Chicago Press, Chicago.

Woodward, F.I., 1987. Stomatal numbers are sensitive to increases in CO_2 concentration from the pre-industrial levels. Nature 327, 617–618.